

Accepted Manuscript

Dynamic interactions between sulfidated zerovalent iron and dissolved oxygen:
Mechanistic insights for enhanced chromate removal

Qianqian Shao, Chunhua Xu, Yahao Wang, Shasha Huang, Bingliang Zhang, Lihui Huang, Dimin Fan, Paul G. Tratnyek



PII: S0043-1354(18)30135-0

DOI: [10.1016/j.watres.2018.02.030](https://doi.org/10.1016/j.watres.2018.02.030)

Reference: WR 13582

To appear in: *Water Research*

Received Date: 22 December 2017

Revised Date: 11 February 2018

Accepted Date: 12 February 2018

Please cite this article as: Shao, Q., Xu, C., Wang, Y., Huang, S., Zhang, B., Huang, L., Fan, D., Tratnyek, P.G., Dynamic interactions between sulfidated zerovalent iron and dissolved oxygen: Mechanistic insights for enhanced chromate removal, *Water Research* (2018), doi: 10.1016/j.watres.2018.02.030.

This is a PDF file of an unedited manuscript that has been accepted for publication. As a service to our customers we are providing this early version of the manuscript. The manuscript will undergo copyediting, typesetting, and review of the resulting proof before it is published in its final form. Please note that during the production process errors may be discovered which could affect the content, and all legal disclaimers that apply to the journal pertain.

Dynamic Interactions between Sulfidated Zerovalent Iron and Dissolved Oxygen: Mechanistic Insights for Enhanced Chromate Removal

Qianqian Shao¹, Chunhua Xu^{1*}, Yahao Wang¹, Shasha Huang¹, Bingliang Zhang¹,
Lihui Huang¹, Dimin Fan^{2*} and Paul G. Tratnyek³

¹ School of Environmental Science and Engineering
Shandong University, Jinan, Shandong, 250100, China

² Oak Ridge Institute for Science and Education Fellow, Office of Superfund
Remediation and Technology Innovation, U.S. Environmental Protection Agency,
Arlington, VA, 22202 USA

³ OHSU-PSU School of Public Health, Oregon Health & Science University
3181 SW Sam Jackson Park Road, Portland, OR 97239

*Corresponding authors:

Email: xuchunhua@sdu.edu.cn, Phone: 86-531-88362586, Fax: 86-531-88364513

Email: fan.dimin@epa.gov, Phone: 703-603-8703

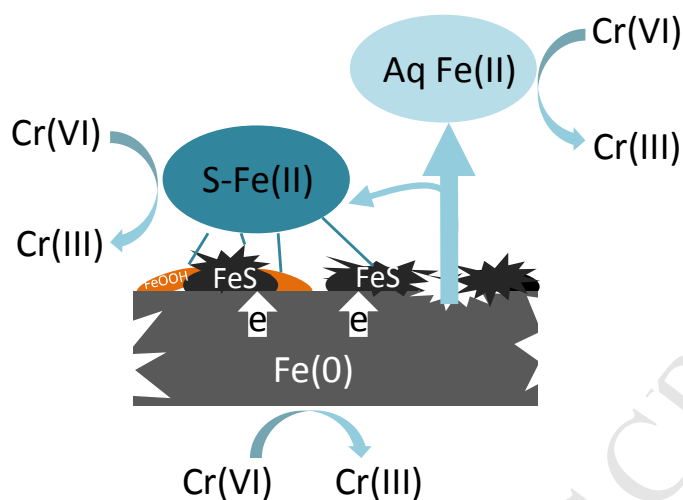
ShaoXuFan2017-FeFeS-Cr-Oxic-MT-vf-clean.docx

Prepared for Water Research

2018-02-15

Abstract

Recent research on contaminant removal by zerovalent iron (ZVI) has evolved from investigating simple model systems to systems that encompass increased dimensions of complexity. Sulfidation and aerobic conditions are two of the most broadly relevant complications. Combining these two, this study investigated the dynamic interactions between sulfidated microscale ZVI and dissolved O_2 , for removal of Cr(VI), a model contaminant for metals and metalloids. The results show that the coupling of sulfidation and oxygenation significantly improves Cr removal, which is attributed to enhanced Fe(II) production that resulted from accelerated corrosion of Fe(0). The Cr(VI) removal rate increased with increasing O_2 saturation from 0% to 100% but showed a bimodal dependence on the S/Fe ratio. At the optimal S/Fe ratio, the ZVI exhibits a highly porous surface morphology, which, according to prior literature on sulfur induced corrosion, promotes corrosion. In addition, a novel time series correlation was developed between aqueous Fe(II) and Cr(VI) based on data collected in the presence and absence of 1,10-phenanthroline, to probe for changes of reductants during the reaction time course. The analysis indicated that Fe(0) was responsible for the initial small amount of Cr(VI) removal, which then transitioned to a phase controlled by surface Fe(II). The slopes of the time series correlations during the latter phase of the reaction vary with experimental conditions but are mostly much higher than the theoretical stoichiometric ratio between Cr(VI) and Fe(II) (i.e., 0.33), indicating that Fe(II) regeneration contributes significantly to Cr removal.



Key words:

Sulfidation, Zerovalent iron, Aerobic, Reductive sequestration, Fe(II) regeneration, Corrosion enhancement

Highlights:

- Sulfidation of ZVI enhances Cr(VI) removal under aerobic conditions.
- Sulfidation and oxygenation enhance corrosion rate of Fe(0).
- Regeneration of surface Fe(II) contributes significantly to Cr(VI) removal.
- S/Fe ratio affects surface morphology of S-ZVI and its corrosion rate.
- Time series correlations were developed to differentiate main reductants for Cr(VI)

1. Introduction

Contaminant removal, especially of metals and metalloids, by iron-based materials is important in a wide range of environmental processes, including biogeochemical transformation of radionuclides in the subsurface (Bargar et al., 2013, Icenhower et al., 2010, McBeth et al., 2011, O'Loughlin et al., 2011, Um et al., 2011), remediation of contaminated groundwater (Bang et al., 2005, Beaulieu and Ramirez, 2013, Crane et al., 2011, Cundy et al., 2008, Puls et al., 1999), and treatment of industrial wastewater (Fu et al., 2014, Li et al., 2014a, Li et al., 2014b, Xu et al., 2012). The relevant types of iron-based reducing materials are mainly zerovalent iron (ZVI) (Cantrell et al., 1995, Sun et al., 2016), followed by amorphous iron monosulfide (FeS) (Gong et al., 2016), as well as a few other iron containing oxides such as magnetite (Crane et al., 2011, Mamindy-Pajany et al., 2011, Powell et al., 2004). The abundance of research using these materials is partly due to their environmental significance, but it also reflects their relatively well-understood physiochemical properties, which make them useful as model systems in studies of the mechanisms, kinetics or capacity, of contaminant removal under a variety of conditions (Coles et al., 2000, Han et al., 2011, Hyun et al., 2012, Jeong et al., 2010b, Li et al., 2017c, Powell et al., 1995, Ramos et al., 2009, Shipley et al., 2010, Yan et al., 2010, Zhang et al., 2013).

Building on the knowledge-base from many detailed studies of the contaminant removal processes by iron based materials, new research has gradually evolved from simple model systems to systems that involve an increasing degree of complexity. This is especially true for ZVI, where complexity has been introduced in various dimensions. Examples include (i) surface and structural modification of ZVI (Li et al., 2012, Xu and Zhao, 2007, Zou et al., 2016); (ii) chemical (Liu et al., 2013a, Tang et al., 2014, Xie and Cwiertny, 2010), magnetic (Feng et al., 2015, Kim et al., 2011, Liang et al., 2015, Liang et al., 2014b), and electrochemical activation of

ZVI (Chen et al., 2012), and (iii) variations of environmental matrix (Dries et al., 2005, Liang et al., 2013, Liu et al., 2013b, Sun et al., 2016). The primary aims of these new developments are to (i) explore improvements to enhance effectiveness of ZVI for contaminant removal and (ii) overcome limitations that may impede the full scale applications of ZVI (e.g., passivation of Fe(0)) (Guan et al., 2015). However, these complexities can result in dynamic and transient behaviors involving reactive species in both aqueous and solid phases, which can reveal new fundamental processes that were not evident in simpler model systems.

One emerging area that has recently attracted a great deal of interest is the sulfidation of ZVI (Fan et al., 2017, Li et al., 2017b), mostly nZVI but recently expanded to include microscale ZVI (mZVI) (Gu et al., 2017, Xu et al., 2016a). The process involves modification of ZVI by a variety of lower valent sulfur compounds, most commonly aqueous sulfide and dithionite to form iron sulfides either on the surface of Fe(0) as mixed with the core material (Fan et al., 2017). Sulfidation was initially used to mimic naturally-occurring microbial sulfate reduction, which can be stimulated by emplacement of ZVI in the subsurface. (Gu et al., 1999, Kirschling et al., 2010, Phillips et al., 2010) More recent studies showed that controlled sulfidation could be an effective strategy to tune the reactive properties of ZVI in favor of a broad range of contaminant removal processes. The benefits identified to date include selective metal sequestration as metal sulfides (as opposed to labile metal oxides) (Fan et al., 2013), enhanced metal adsorption capacity (Su et al., 2015), increasing reactivity and selectivity with organic contaminants (e.g., trichloroethene (TCE)) (Fan et al., 2016, Han and Yan, 2016, Kim et al., 2013, Rajajayavel and Ghoshal, 2015), and enhanced reactivity with emerging contaminants that are recalcitrant to nZVI (Cao et al., 2017, Li et al., 2016, Li et al., 2017a). Collectively, these studies demonstrate

the diverse and important roles of sulfidation in enhancing contaminant transformation and sequestration, either directly or indirectly.

Another prominent development is the expansion of ZVI applications from anaerobic conditions—which mainly applies to groundwater remediation—to aerobic conditions in order to simulate industrial wastewater treatment for metals and organics (Liang et al., 2015, Xu et al., 2016b, Xue et al., 2013). Although conventional wisdom predicts that dissolved oxygen inhibits reductive dehalogenation by ZVI, more recent studies have suggested oxygen can promote contaminant transformation/sequestration by ZVI under some circumstances. For organic contaminants, the activation of molecular oxygen by ZVI has long been recognized as a primary mechanism, (Joo et al., 2005, Keenan and Sedlak, 2008, Lee, 2015, Mu et al., 2017), whereas the beneficial effects for metals and metalloids mainly arise from aerobic corrosion of Fe(0), which either generates additional Fe(II) that serves as a reductant or enhances contaminant sorption and subsequent interfacial electron transfer via iron oxides on the surface of Fe(0) (Qin et al., 2016, Qin et al., 2017, Yoon et al., 2011).

Application of sulfidation for contaminant removal under aerobic conditions has received very little attention so far, but it is expected to grow following the similar path as ZVI. For sulfidated ZVI, the effects of oxygen can bring additional complexity to the system because FeS may also be oxidized in addition to all of the other reactions that could occur in the ZVI system, and the presence of FeS may directly affect the corrosion of Fe(0), and subsequently the production of secondary reductants, such as Fe(II). (Zheng et al., 2015) Although oxidation of FeS has been extensively studied and well understood, the majority of the studies to date concern oxidative remobilization (rather than sequestration) of metals and metalloids that may result from the oxidation of FeS (Bi and Hayes, 2014, Bi et al., 2013, Jeong et al., 2010a). To date, mixed

102 results have been reported on the effects of sulfidated ZVI for contaminant removal under
103 aerobic conditions. Du et al. (2016) showed that the presence of oxygen slightly inhibited the
104 sequestration of chromate by sulfidated nZVI, whereas Xu et al. (2016a) reported fast
105 decolorization of Orange I by sulfidated ZVI under aerobic conditions, although they did not
106 directly compare these results with anaerobic conditions. Nevertheless, neither study has
107 specifically examined the dynamic and transient oxidation processes of sulfidated ZVI and their
108 effects on contaminant transformation.

109 The goal of the present study is to fill this data gap by systematically characterizing
110 contaminant removal by sulfidated ZVI under aerobic conditions. Compared to prior sulfidation
111 work that mostly used laboratory synthesized nZVI, commercially available microscale ZVI was
112 selected here to further expand the family of sulfidated materials. Likewise, for contaminant, we
113 selected the group of metals and metalloids (as opposed to organics), which have been less
114 commonly studied in prior sulfidation research. Specifically, chromate was chosen as a model
115 contaminant because of (i) its prevalence and high toxicity (Gheju, 2011, Ponder et al., 2000);
116 and (ii) more importantly, the relatively well-understood redox behavior of Cr(VI) and the
117 slow/negligible reoxidation of Cr(III) by dissolved oxygen (Gheju, 2011, Rai et al., 1989). The
118 latter ensures unambiguous analysis of the kinetics of contaminant sequestration in such a
119 complex system that likely involves multiphase reductants in solid phase, redox disequilibrium
120 in aqueous phase, and dynamic interactions between the two. To achieve that, we employed a
121 suite of solution chemistry and solid phase characterization approaches and developed a novel
122 time series correlation analysis method based on the 1,10-phenanthroline assay to examine
123 reductive sequestration of Cr(VI) by sulfidated ZVI under aerobic conditions.

2. Experimental Section

2.1. Chemical reagents

Analytical grade sodium sulfide (Na_2S), sodium sulfate (Na_2SO_4), and potassium dichromate (K_2CrO_4) purchased from Tianjin Kermel Chemical Reagent Co. (Tianjin). Acetic acid (HAc), sodium acetate (NaAc) were purchased from Sigma-Aldrich Co. LLC. (China). All reagents were used as received without further purification. Stock solutions of K_2CrO_4 (1000 mg/L) were prepared by dissolving K_2CrO_4 with ultrapure deionized water. The granular ZVI used in this study was obtained from Alfa Aesar Chemical Co., Ltd. (China) (Alfa iron) and Beijing Enviro-Chem Environmental Technology Co., Ltd. (Beijing, P.R. China) (Beijing iron).

2.2. Sulfidation

Sulfidation was carried out in 250 mL glass serum bottles. Each bottle was filled with 250 mL acetic acid-sodium acetate buffer solution at pH 6, and then deoxygenated by bubbling N_2 for at least 30 minutes. After deoxygenation, ZVI powder (1 g) was added into the bottle, which was immediately crimp-sealed with an aluminum crimp-top. The bottles were put in a rotary water bath shaker at 120 rpm and 25 ± 0.2 °C for 10 min to disperse the ZVI particles and release Fe(II) to solution. Different volumes of Na_2S stock solutions (1 M) were injected into the serum bottles, to achieve S/Fe molar ratios of 0.028, 0.042, 0.056, 0.070, 0.084, 0.112. After mixing for 12 h, the solids were collected by vacuum filtration, and the filtered particles were freeze-dried at -50 °C for 2 hr. To differentiate the ZVI and sulfidated ZVI, we designated the latter as S-ZVI in consistency with the recent terminology proposed for ZVI sulfidated by aqueous-solid approach (Fan et al., 2017)

2.3. Batch Experiments.

Batch experiments of Cr(VI) removal by ZVI and S-ZVI were performed in 1 L beakers open to air and at room temperature ($25 \pm 1^\circ\text{C}$). In most cases, an aliquot of S-ZVI or ZVI was added to 1 L of 5 mg/L Cr(VI) solution with 1 mM Na_2SO_4 as background electrolyte. Some experiments were unbuffered with the initial pH adjusted to 5.0. The rest used acetate buffer to control pH around 5. In order to investigate the effect of dissolved oxygen, mixed gas of nitrogen and oxygen passed through the aeration tube into the flask reactor continuously. The volume percentage (V%) of oxygen was controlled at 0%, 2.5%, 5.0%, 20%, 50% and 100% in the mixed gas by variable-area flow meters and the flow rate of the mixed gas was maintained at 0.5 L/min. The solution was mixed at 400 rpm with a mechanical stirrer, and an aliquot of sample (5 mL) was periodically withdrawn, filtered with 0.22 μm membrane filters, and acidified immediately for analysis of various aqueous species.

2.4. Analytical Methods.

Aqueous Cr(VI) was measured using a UV-Vis spectrophotometer (UV 1901 PC, Shanghai Aoxi Scientific Instrument Co., China) (absorbance measured at 540 nm). Ferrous iron (Fe(II)) was determined using the phenanthroline spectrophotometric method. Total iron (Fe_{tot}) was analyzed by inductively coupled plasma atomic emission spectroscopy (ICP-AES). In addition, pH, dissolved oxygen (DO) and oxidation-reduction potential (Eh) of the reaction system were monitored using commercial combination electrodes (DO-957, 501 ORP, E-201-C28 pH, INESA Scientific Instrument Co., Ltd, China). The Eh electrode was calibrated at quinhydrone solution and the data was adjusted to the standard hydrogen electrode (SHE) scale by adding 193.5 mV.

2.5. Solid phase characterization

The solid samples were collected on membrane filters (0.22 μm), washed with deionized water, freeze-dried under vacuum at $-50\text{ }^{\circ}\text{C}$ for 2 h, and stored in zip-lock plastic bags until analysis. S-ZVI with selected S/Fe ratio at reaction time 0 min, 30 min, 120 min and ZVI (0 min) were characterized by X-ray photoelectron spectroscopy (XPS) (ESCALAB 250Xi, Thermo Fisher Scientific, USA) to analyze the surface mineralogy. XPS was conducted with Al K α radiation and the power at 150 W. The binding energies were calibrated to the C 1s peak at 284.8 eV and survey scans were performed with 1.0 eV step, high resolution scans with 0.05 eV step. Scanning electron microscopy (SEM) (Quanta F250, FEI, USA) coupled with energy dispersive X-ray spectroscopy (EDS) (Genesis, EDAX, USA) was additionally applied to characterize the material morphology and elemental composition. Specific surface areas of unmodified ZVI and S-ZVI samples were determined by nitrogen adsorption using the Brunauer–Emmett–Teller (BET) method (TriStar II 3020, USA). Surface roughness of the samples was measured by atomic force microscopy using a Dimension 3100 AFM with a Nanoscope V controller in standard tapping mode (Icon Bruker, GER). The samples were prepared by dispersing onto black phosphorus nano sheets in ethanol and drop casting over cleaned Si substrates.

3. Results and Discussion

3.1. Cr removal by S-ZVI under Aerobic and Anaerobic Conditions.

The kinetics of Cr(VI) removal by ZVI and S-ZVI was examined under both aerobic and anaerobic conditions (**Fig. 1**). With untreated ZVI, little or no Cr(VI) removal was observed under both anaerobic and aerobic conditions. These results suggest the high degree of surface passivation of the type of ZVI used in this study, which is mainly due to the indigenous iron oxide layer on this material (as indicated by the XPS data (**Fig. S1**)), but may also be due to precipitation of Cr(III) in the early stages of reaction, which would further passivate ZVI. Using sulfidated ZVI, higher Cr removal was achieved, which is consistent with the favorable effects of sulfidation reported by prior literature on metal removal by sulfidated nZVI under anaerobic conditions (Du et al., 2016, Fan et al., 2013, Su et al., 2015). In addition, the presence of oxygen

greatly improved Cr(VI) removal compared to anaerobic conditions (complete removal of 5 mg/L Cr(VI) was achieved within 40 min in the presence of oxygen). Similar results were observed for the Beijing ZVI although the improvement by sulfidation under aerobic conditions was not as significant as with Alfa ZVI (**Fig. S2**).

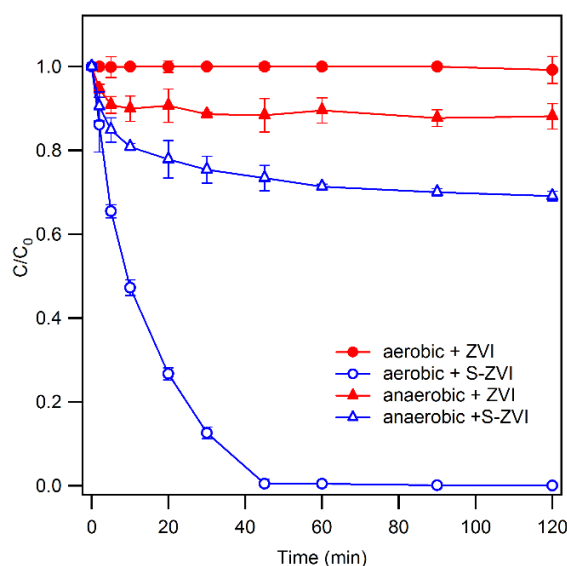


Fig. 1. Effects of sulfidation and oxygen on Cr(VI) removal by ZVI. Reaction conditions: 0.2 g/L ZVI or S-ZVI (S/Fe = 0.056), 5 mg/L Cr(VI), pH_{ini} = 5 (unbuffered), RPM = 400 and 1 mM Na₂SO₄.

Enhanced Cr(VI) removal by ZVI under oxic condition has been reported by several prior studies (Feng et al., 2015, Qin et al., 2016, Yoon et al., 2011). The enhancement was attributed to formation of Fe(III) and Cr(III) precipitates under oxic conditions, which are less passivating than the one formed under anaerobic conditions (Yoon et al., 2011) or enhanced Fe(0) corrosion by oxygen (Qin et al., 2016), which produces additional Fe(II). It has been reported that the presence of oxygen does not affect Cr(VI) reduction by Fe(II) under a wide range of pHs (Fendorf and Li, 1996). The significant difference in Cr(VI) removal between anaerobic and aerobic conditions observed in this study seems to indicate that a large quantity of additional reductant was generated from S-ZVI under aerobic conditions, which aligns more closely with

the second explanation. However, the most compelling evidence that usually is used to support the latter argument—the absence of measurable aqueous Fe(II) until aqueous Cr(VI) concentration approached zero—was not observed here. **Fig. S3A** shows that, for S-ZVI, both the presence and absence of Cr(VI) gave little production of Fe(II) (up to 1 mg/L). Parallel pH measurements showed a rapid increase from 5 to circumneutral range (**Fig. S3C**), suggesting that little aqueous Fe(II) measured might be due to Fe(II) oxidation or formation of sorbed Fe(II), both favored at high pH.

To verify the effects of pH on release of Fe(II), additional experiments were conducted at pH 5 buffered by NaAc-HAc. At constant pH of 5, little aqueous Fe(II) was produced until Cr(VI) removal approached completion ($t = 20$ min in this case) (**Fig. 2**), which is similar to Fe(II) profiles reported by several prior studies (Feng et al., 2015). The rate of Cr removal was faster than in the unbuffered treatment, which is consistent with many previous studies showing that lower pH accelerates Cr(VI) removal in ZVI system due to faster corrosion of Fe(0) (Alowitz and Scherer, 2002, Gheju, 2011, Gheju and Iovi, 2006). To further examine and quantify the role of Fe(II) in Cr(VI) removal, we added 1,10-phenanthroline into the reaction, which is an Fe(II) complexing ligand. Due to stronger complexation with Fe(II) than Fe(III), 1,10-phenanthroline increases the redox potential of Fe(II)/Fe(III) couple (Galicia et al., 1990), thus making Fe(II) unavailable for Cr(VI) reduction (Buerge and Hug, 1998). This protocol has been used in a couple of recent studies to prove significant contribution of Fe(II) to Cr(VI) removal in ZVI relevant systems under anaerobic conditions (Du et al., 2016, Mu et al., 2015, Zhou et al., 2008). Consistent with those studies, our data shows that the addition of 1,10-phenanthroline caused significant inhibition of Cr(VI) removal, but Fe(II) production was not inhibited initially (**Fig. 2**). Comparing the two cases, it appears that the amount of Fe(II)

complexed by 1,10-phenanthroline is responsible for the difference in Cr(VI) removal between aerobic and anaerobic conditions.

The difference in Fe(II) production at 20 min with and without 1,10-phenanthroline (0.095 mM), however, only accounts for ~40% of Cr(VI) removal difference observed at that time point (0.075 mM), according to the reaction stoichiometry between Fe(II) and Cr(VI). A control experiment showed that the Fe(II)-phenanthroline complex is stable under our experimental conditions (i.e., pH 5, buffered, and aerobic) (**Fig. S4**), so underestimation of Fe(II) in the presence of 1,10-phenanthroline due to oxidation is unlikely. It has also been reported that 1,10-phenanthroline might act as a corrosion inhibitor for steel, thus lowering Fe(II) production (Banerjee and Misra, 1989). However, measurement of Fe(II) evolution during oxidation of S-ZVI in the presence and absence of 1,10-phenanthroline showed negligible differences (**Fig. S5**). These results indicate that unaccounted reductants must be responsible for Cr(VI) reduction.

In our system, possible reductants other than Fe(II) include primary reductants such as Fe(0), FeS, and secondary reductants such as atomic hydrogen and S(-II) that result from reaction or decomposition of the primary reductants. However, the primary reductants are subject to oxidation by O₂ and therefore may not provide continuous removal of Cr(VI). The contributions of the secondary reductants other than Fe(II) should not be affected by the addition of 1,10-phenanthroline. As a result, the only possibility left is regeneration of surface Fe(II) from Fe(III) by Fe(0) (Scherer et al., 1998). The regenerated Fe(II) may not be detected by the phenanthroline assay because Fe(III) would not be produced for regeneration due to complexation of Fe(II)-phenanthroline. Surface Fe(II) has been proposed to play a major role in Cr(VI) removal by oxide-coated nZVI under anoxic conditions (Mu et al., 2015) or by Fe(II)-sorbed minerals (Buerge and Hug, 1999). Reduction of surface Fe₂O₃ by the Fe(0) core was

suggested as one of the two major routes for producing surface Fe(II) (Mu et al., 2015). Given higher electron conductivity of FeS than oxides, similar electron transfer process from core to surface is highly plausible in our system.

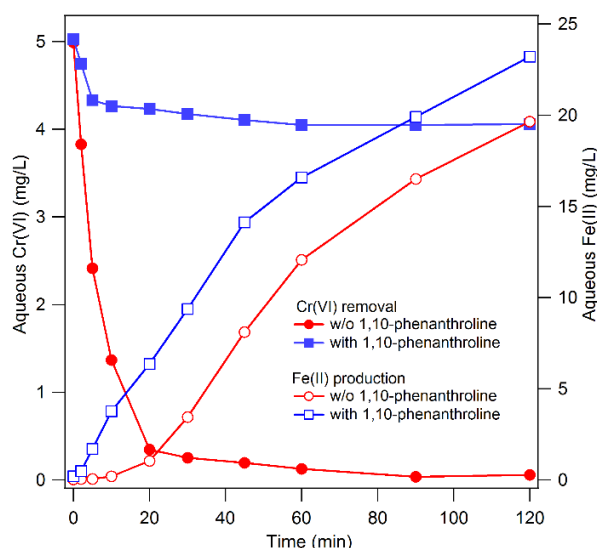
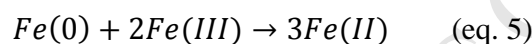
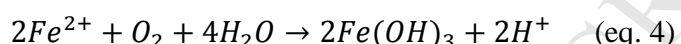
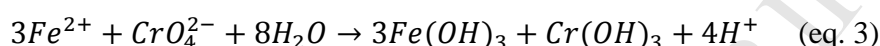
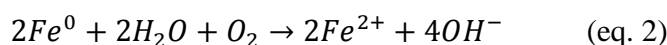
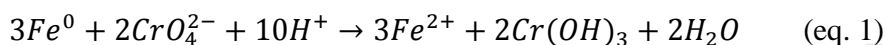


Fig. 2. Cr(VI) removal by S-ZVI and the release of Fe(II) from S-ZVI in the absence or presence of 1,10-phenanthroline. Reaction conditions: 0.2 g/L S-ZVI (S/Fe = 0.056), 5 mg/L Cr(VI), aerobic, buffered at pH 5 by NaAC-HAC, RPM = 400 and 2 mM 1,10-phenanthroline if added.

Conceptually, the contribution of regenerated Fe(II) to Cr(VI) removal is controlled by the relative rates of three processes that proceed concurrently: (i) production of Fe(II) from Fe(0) (eq. 1 and eq. 2); (ii) oxidation of Fe(II) by Cr(VI) or O₂ to form Fe(III) (eq. 3 and eq. 4); and (iii) reduction of Fe(III) by Fe(0) that regenerates Fe(II) (eq. 5). Therefore, a qualitative hypothesis can be made that enhanced rates of Fe(II) production may reduce the contribution of regenerated Fe(II) to Cr(VI) removal. The contribution of regenerated Fe(II) to Cr(VI) reduction may also be affected by the dynamic characteristics of surface FeS layer upon oxidation because, the phases on the material surface affect both Fe(II) production and regeneration, as both processes involve transfer of reactive species across the surface layer. To further test these

hypotheses, experiments were conducted to examine the effects of oxygen concentration and S/Fe ratio on Cr(VI) removal.



3.2. Effects of Oxygen Concentration on Cr(VI) Removal.

The effects of oxygen concentration on Cr(VI) removal were evaluated for S/Fe ratio of 0.056 in unbuffered solution. **Fig. 3A** shows that increasing O₂ concentration from 0% to 100% enhanced the rate of Cr(VI) removal in the absence of 1,10-phenanthroline. In the presence of 1,10-phenanthroline, increasing O₂ concentration led to faster and greater Fe(II) production (**Fig. 3B**), again supporting that Cr(VI) removal rate is largely dependent on the Fe(II) availability. To further quantify the relationship between the rate of Fe(II) production and the rate of Cr(VI) reduction, aqueous Cr(VI) concentrations *in the presence* and *absence* of 1,10-phenanthroline were plotted against aqueous Fe(II) concentration measured *in the presence* of 1,10-phenanthroline (**Fig. 3C**). This kind of binary time series correlation analysis is derived from our previous work, which has been proven to be diagnostic in identifying and distinguishing dominant controlling processes for contaminant removal. (Liang et al., 2014a, Xu et al., 2016a, Xu et al., 2016b)

The correlation analysis in **Fig. 3C** clearly shows that the presence and absence of 1,10-phenanthroline produced two distinct groups of time series data. In the presence of 1,10-phenanthroline, all of the data, regardless of O₂ concentration, appear to fall on a single curve

that has two segments. The first segment accounts for majority of the Cr(VI) reduction. Since Fe(II) complexed by 1,10-phenanthroline is unavailable to reduce Cr(VI), this initial reduction of Cr(VI) must be caused by the primary reductants Fe(0) and/or FeS. This conclusion is additionally supported by solution chemistry data shown in **Fig. S3**. For S-ZVI both in the presence and absence of Cr(VI), aqueous Fe(II) rapidly increased to slightly less than 1 mg/L at the 2-min sampling point (**Fig. S3A**), suggesting that Fe(II) was generated by Fe(0) oxidation (eq. 1 and 2). However, the presence of Cr(VI) results in less decrease in DO than in the absence of Cr(VI) (**Fig. S3B**), suggesting that Cr(VI) reduction competes with O₂ reduction for Fe(0).

In the absence of 1,10-phenanthroline, close inspection of the data shows that correlation between Cr(VI) and Fe(II) has three distinct segments for all O₂ concentrations. The initial phase appears to have similar slopes for all O₂ concentrations (as represented by the linear fitting for 0% O₂ data), which is similar to the effect of O₂ seen in the presence of 1,10-phenanthroline, again suggesting that the primary reductants control the initial reduction of Cr(VI). The fact that the initial phase in the absence of 1,10-phenanthroline produced more Cr(VI) reduction than in the presence of 1,10-phenanthroline is likely because additional Fe(II) generated by Cr(VI) reduction by Fe(0) (eq. 2) can further reduce Cr(VI) without 1,10-phenanthroline (eq. 3).

Compared to the first segment in the time series correlations for data without phenanthroline, the slope of the second segment shows a subtle but clear divergence with increasing oxygen concentration (**Fig. 3C**). The transition between these segments indicates that the dominant reductant has switched to Fe(II). The slopes of the second segments for all O₂ concentrations are much greater than the theoretical stoichiometric ratio between Cr(VI) and Fe(II), suggesting that Fe(II) regeneration is an important contributor to Cr(VI) reduction. The slope becomes less steep with increasing O₂ concentration, indicating less contributions from

regenerated Fe(II) to Cr(VI) removal, due to faster Fe(II) production at high O₂ concentration (Fig. 3B). However, one potential limitation to this analysis on this particular dataset is that there was a pH difference between the presence and absence of 1,10-phenanthroline in unbuffered system. The addition of 1,10-phenanthroline stabilized pH around 5 (data not shown), whereas without adding 1,10-phenanthroline, the pH rose to circumneutral range. As high pH typically lowers the oxidation rate of Fe(0) and favors formation of sorbed Fe(II) (Sedlak and Chan, 1997), the aqueous Fe(II) measured in the presence of 1,10-phenanthroline may overestimate the actual Fe(II) concentration in the absence of 1,10-phenanthroline. Nevertheless, this should not change the qualitative conclusion that increasing O₂ concentration enhances Fe(II) production and, therefore, decreases the contribution of regenerated Fe(II) to Cr(VI) removal. The transition from the second segment to the tail phase likely indicates decreasing contribution of regenerated Fe(II) to Cr(VI) reduction as the slope becomes significantly less steep.

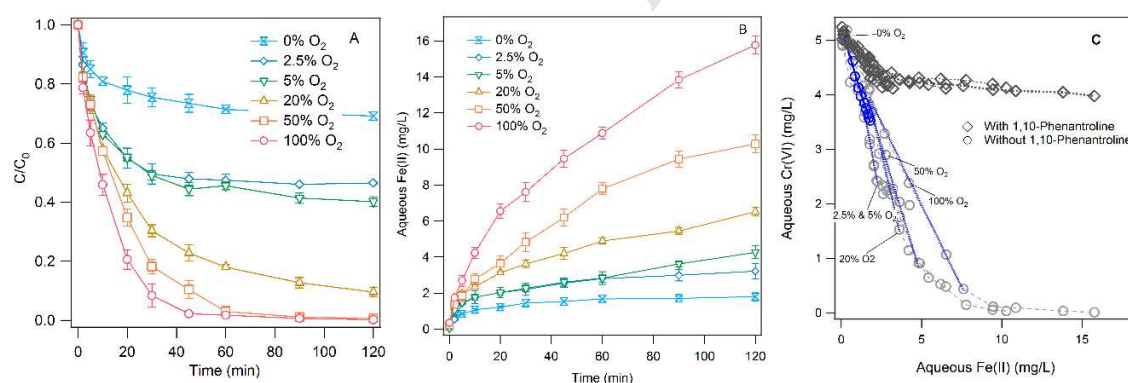


Fig. 3. (A) Cr(VI) removal by S-ZVI under different oxygen concentrations. (B) The release of Fe(II) from S-ZVI during reaction with Cr(VI) under different oxygen concentration in presence of 1,10-phenanthroline. (C) Aqueous Cr(VI) concentration in the absence of 1,10-phenanthroline vs. aqueous Fe(II) concentration in the presence of 1,10-phenanthroline. Reaction conditions: 0.2 g/L S-ZVI (S/Fe = 0.056), 5 mg/L Cr(VI), pH_{ini} = 5 (unbuffered), RPM = 400, 1 mM Na₂SO₄ and 2 mM 1,10-phenanthroline if added.

3.3. Effects of S/Fe ratio on Cr(VI) Removal

A bimodal pattern was observed for Cr(VI) removal with increasing S/Fe ratio (**Fig. 4**), which is similar to what has been reported in several prior sulfidation studies (Fan et al., 2013, Rajajayavel and Ghoshal, 2015). In this case, the maximum removal kinetics was achieved at S/Fe = 0.056, and the removal capacity followed the same trend. Three intermediate S/Fe ratios (0.042, 0.056, and 0.070) resulted in nearly 100% removal after 120 min reaction, but both low and high S/Fe ratios showed significant tailing and incomplete Cr removal by 120 min. Subsequent measurement of aqueous Fe(II) in the presence of 1,10-phenanthroline at various S/Fe ratios also showed a bimodal pattern that is consistent with the Cr removal data (**Fig. 4B**). Lower Fe(II) production at high S/Fe ratios provides strong evidence that the main source of Fe(II) is not from oxidative dissolution of FeS, but instead is supplied by the dynamic corrosion process of the Fe(0) core. The variability of Fe(II) production and Cr(VI) removal with S/Fe ratio indicates that surface iron sulfide plays a significant role in affecting the corrosion rate of the underlying Fe(0).

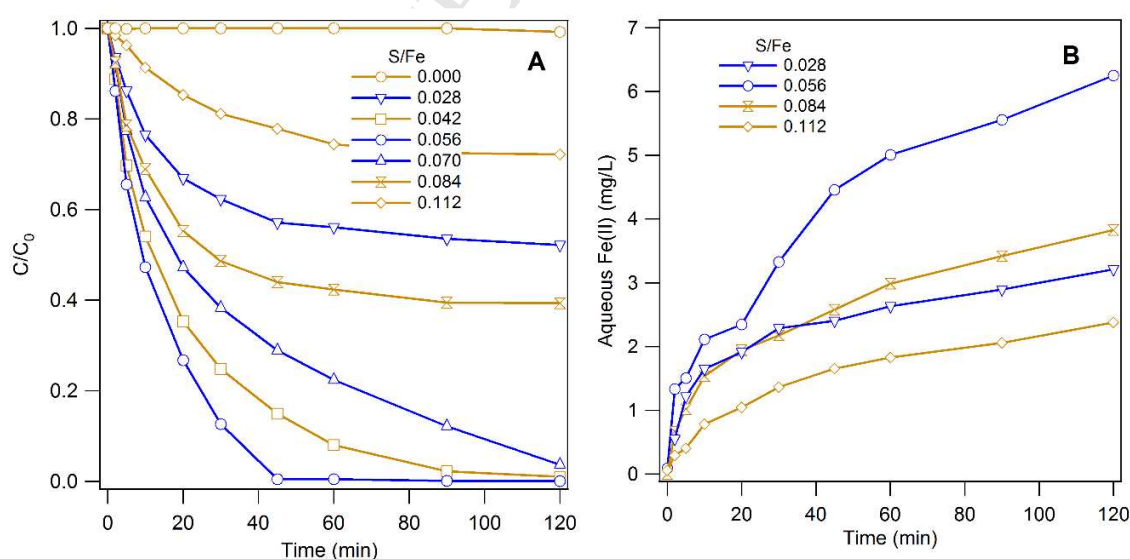


Fig. 4. (A) Cr(VI) removal by S-ZVI of different S/Fe ratios. (B) Release of Fe(II) during Cr(VI) reaction with S-ZVI of different S/Fe ratios in presence of 1,10-phenanthroline. Reaction

conditions: 0.2 g/L S-ZVI, 5 mg/L Cr(VI), aerobic, $\text{pH}_{\text{ini}} = 5$ (unbuffered), RPM = 400, 1 mM Na_2SO_4 and 2 mM 1,10-phenanthroline if added.

The above interpretation supports one of the key themes in our recent review on sulfidation (Fan et al., 2017). Although the existing environmental literature generally concludes that sulfidation inhibits corrosion of Fe(0) (Fan et al., 2016, Han and Yan, 2016, Rajajayavel and Ghoshal, 2015), extensive prior work on sulfur induced corrosion has shown both inhibitory and promoting effects and suggested the transition between the two is finely controlled by environmental variables (Bai et al., 2016, Enning and Garrelfs, 2014, Newman et al., 1992). For example, it has been shown that increasing sulfide concentration could change the effects on corrosion rate of steel from inhibition to promotion, then back to inhibition (Sun and Nešić, 2009) (Zheng et al., 2015). The inhibition at low sulfide concentration is due to the formation of a dense base layer of FeS at very low sulfide concentration. As sulfide concentration increases, the transition from inhibition to promotion arises because from precipitation of secondary FeS that is highly porous, which compromise the dense base layer and induces localized corrosion.

The second inhibition phase at higher sulfide concentration is attributed to the sealing of open pores by further formation of FeS. The transition from the second to the third phases seen in previous studies of corrosion under sulfidic conditions is consistent with the kinetic data in this study, and is further supported by scanning electron micrographs (SEMs) of S-ZVI with different S/Fe ratios (**Fig. 5**). The S-ZVI prepared at S/Fe = 0.056 shows a highly porous surface morphology that is distinct from the materials prepared at both lower and higher S/Fe ratios. Despite EDS showing higher S content at S/Fe of 0.084 (**Fig. S6**), its SEM shows fewer and smaller pores than that of S/Fe of 0.056 (**Fig. 5**), suggesting that additional FeS filled the open pore space. Additional measurements of surface roughness and surface area showed the same

bimodal patterns with S/Fe ratio (**Fig. 5E and Table S1**), all of which is consistent with the rates of Fe(II) production and Cr(VI) removal. This confirms that the surface morphology of S-ZVI controls the corrosion of underlying Fe(0), and this affects the production of Fe(II) and subsequent reduction of Cr(VI).

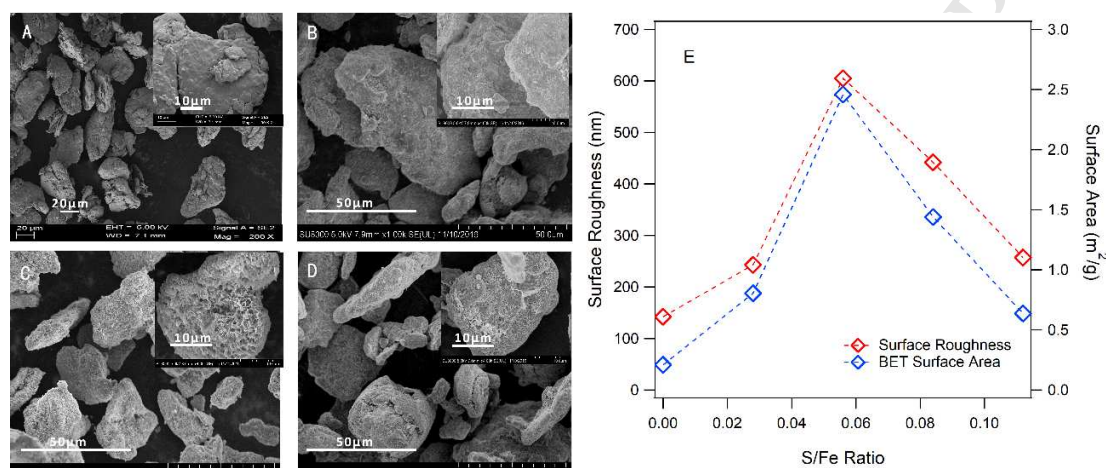


Fig. 5. SEM analysis for S-ZVI: (A) untreated ZVI, (B) S-ZVI (S/Fe = 0.028) (C) S-ZVI (S/Fe = 0.056), (D) S-ZVI (S/Fe = 0.084). (E) Surface roughness and surface area measurements of S-ZVI at different S/Fe ratios.

A time series correlation similar to **Fig. 3C** was also performed on data collected with different S/Fe ratios. To eliminate the pH effects discussed in **Fig. 3C**, an additional set of experiments was conducted in buffered solution. Comparison between the time series correlations in buffered (**Fig. 6A**) and unbuffered (**Fig. 6B**) systems showed that buffering did not change the bimodal dependence of Cr(VI) removal on S/Fe ratio observed in unbuffered system, but buffering gave faster or more complete Cr(VI) removal at all S/Fe ratios (**Fig. 6**). This is probably due to the lower pH maintained in the buffered systems, which results in more Fe(II) production (e.g., Fe(II) production for S/Fe of 0.056 reached nearly 25 mg/L in buffered system (**Fig. S7B**)). In general, the slopes of the correlations in the presence of buffer are less steep compared to those in the absence of buffer, consistent with higher Fe(II) production in the

400 presence of buffer (indicative of less contribution of regenerated Fe(II)). However, within each
401 dataset, the time series correlations between aqueous Cr(VI) and Fe(II) appear to not differ by
402 much in terms of the respective slopes of each segment, which is in contrast with the correlations
403 obtained for the effect of oxygen, which showed the differences in the slopes of the second
404 segment discussed above (**Fig. 3C**). The opposite effects of S/Fe ratio and oxygen level on these
405 correlations are difficult to explain with our existing data, but possibly reflects how internal (i.e.,
406 S/Fe ratios) and external (i.e., oxygen levels) variables may influence the system dynamics
407 differently. An example showing how different oxygen levels affect surface morphology of S-
408 ZVI is shown in **Fig. S8** for S/Fe ratio of 0.056. It can be seen that in the absence of oxygen the
409 porous surface feature of the unreacted S-ZVI completely disappeared after reaction with Cr(VI)
410 for 120 min, but the morphology preserved at oxygen level of 20%. Thus, it is plausible that the
411 morphological changes at different oxygen levels may affect the relative ratio between Fe(II)
412 production and regeneration. On the other hand, the ratio between the two may be less sensitive
413 to the material properties determined by S/Fe ratios than to oxygen. Further testing and
414 validation of this hypothesis is beyond the scope of this work, but might be done using
415 electrochemical methods to provide high-resolution temporal characterization of changes in the
416 surface layers and the redox properties of these phases (Turcio-Ortega et al., 2012).

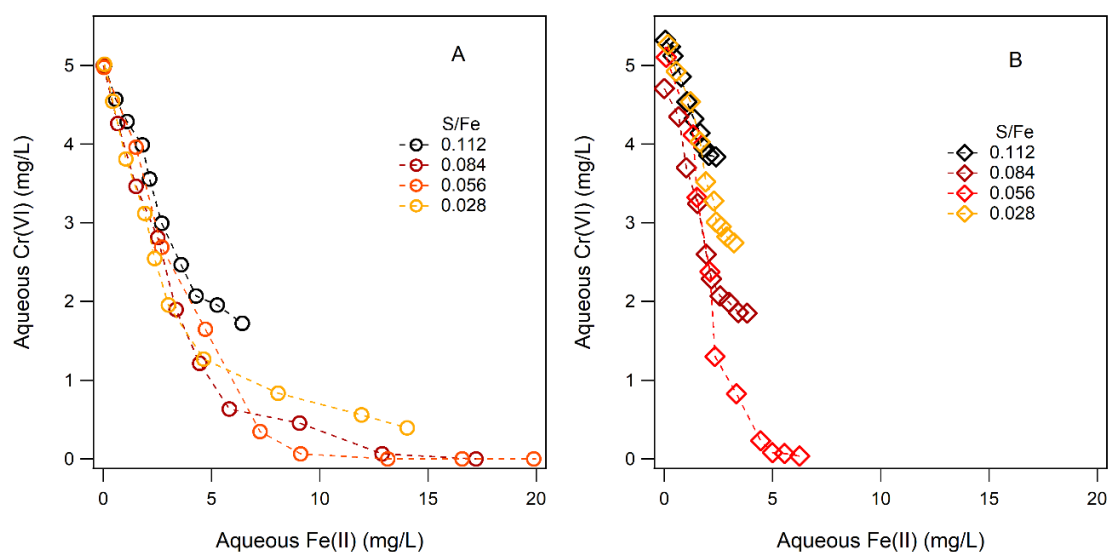


Fig. 6. Aqueous Cr(VI) concentration in the absence of 1,10-phenanthroline vs aqueous Fe(II) concentration in the presence of 1,10-phenanthroline under various S/Fe ratios in (A) Buffered at pH 5 by NaAC-HAC and (B) unbuffered systems. Reaction conditions: 0.2 g/L S-ZVI, 5 mg/L Cr(VI), aerobic, $\text{pH}_{\text{ini}} = 5$, RPM = 400 and 2 mM 1,10-phenanthroline if added.

4. Conclusions

The combination of sulfidation and aerobic conditions used in this study provides new insights into the effects of both these factors, and the first data on their interactions. The approach taken in this study also expands both the scope of ZVI type and contaminant probe compound, which to date have mostly focused on nZVI and organics. Most importantly, the results of this study expands the diversity of the underlying mechanisms that are responsible for the benefits of sulfidation, which previously included only the formation of metal sulfides for metals and metalloids and improved reactivity and selectivity due to inhibited corrosion of Fe(0) for organics. The enhanced removal of Cr(VI) shows that benefits of sulfidation can be achieved for metals or metalloids that do not form stable sulfide phases. The enhanced corrosion by sulfidation--although opposite the effect that is usually seen with nZVI, which involves enhance dechlorination by inhibiting corrosion--actually reflect a broad spectrum of the dynamic and complex effects of sulfur on corrosion of Fe(0). The correlation between surface morphology and

the rates of Fe(II) production and Cr(VI) removal at different S/Fe ratios provides strong evidence for the fundamental linkage between corrosion of Fe(0) and contaminant removal processes.

In addition, the present work further develops the methods of (i) correlation analysis using time series data, in this case of Fe(II) and Cr(VI), and (ii) controlling availability of Fe(II) by addition of 1,10-phenanthroline. While multiple parallel reactions make it impossible to quantify all of the individual reactions in our system, the combination of method innovations used in this study allowed qualitative identification of three phases where Cr reduction are controlled by reductants of different phases. In addition, deviation of the slope of the correlation from the theoretical stoichiometric ratio between Fe(II) and Cr(VI) provides a diagnostic indicator to evaluate the relative contributions of aqueous Fe(II) and regenerated Fe(II) to Cr(VI) removal. This approach is expected to be applicable to other metals and metalloids, for which Fe(II) is expected to play a major role in contaminant sequestration.

ACKNOWLEDGMENTS

The primary support of this research was the Natural Science Foundation of Shandong Province, China (No. ZR2016EEM50) and Shandong Key Scientific and Technological Development Plan of China (2017GSF17108). Some aspects of the data analysis and interpretation were supported by the U.S. Department of Defense, Strategic Environmental Research and Development Program (SERDP, Award Number ER-2308).

Appendix A. Supplementary Data

Supplementary data related to this article can be found

References

- Alowitz, M.J. and Scherer, M.M. (2002) Kinetics of nitrate, nitrite, and Cr (VI) reduction by iron metal. *Environ. Sci. Technol.* 36(3), 299-306.
- Bai, P., Liang, Y., Zheng, S. and Chen, C. (2016) Effect of amorphous FeS semiconductor on the corrosion behavior of pipe steel in H₂S-containing environments. *Industrial & Engineering Chemistry Research* 55(41), 10932-10940.
- Banerjee, S. and Misra, S. (1989) 1, 10,-phenanthroline as corrosion inhibitor for mild steel in sulfuric acid solution. *Corrosion* 45(9), 780-783.
- Bang, S., Korfiatis, G.P. and Meng, X. (2005) Removal of arsenic from water by zero-valent iron. *J. Hazard. Mater.* 121(1), 61-67.
- Bargar, J.R., Williams, K.H., Campbell, K.M., Long, P.E., Stubbs, J.E., Suvorova, E.I., Lezama-Pacheco, J.S., Alessi, D.S., Stylo, M. and Webb, S.M. (2013) Uranium redox transition pathways in acetate-amended sediments. *Proceedings of the National Academy of Sciences* 110(12), 4506-4511.
- Beaulieu, B. and Ramirez, R.E. (2013) Arsenic remediation field study using a sulfate reduction and zero-valent iron PRB. *Groundwater Monitoring & Remediation* 33(2), 85-94.
- Bi, Y. and Hayes, K.F. (2014) Surface passivation limited UO₂ oxidative dissolution in the presence of FeS. *Environ. Sci. Technol.* 48(22), 13402-13411.
- Bi, Y., Hyun, S.P., Kukkadapu, R.K. and Hayes, K.F. (2013) Oxidative dissolution of UO₂ in a simulated groundwater containing synthetic nanocrystalline mackinawite. *Geochim. Cosmochim. Acta* 102, 175-190.
- Buerge, I.J. and Hug, S.J. (1998) Influence of organic ligands on chromium (VI) reduction by iron (II). *Environ. Sci. Technol.* 32(14), 2092-2099.
- Buerge, I.J. and Hug, S.J. (1999) Influence of mineral surfaces on chromium (VI) reduction by iron (II). *Environ. Sci. Technol.* 33(23), 4285-4291.
- Cantrell, K.J., Kaplan, D.I. and Wietsma, T.W. (1995) Zero-valent iron for the in situ remediation of selected metals in groundwater. *J. Hazard. Mater.* 42(2), 201-212.
- Cao, Z., Liu, X., Xu, J., Zhang, J., Yang, Y., Zhou, J., Xu, X. and Lowry, G.V. (2017) Removal of antibiotic florfenicol by sulfide-modified nanoscale zero-valent iron. *Environ. Sci. Technol.* 51(19), 11269-11277.
- Chen, L., Jin, S., Fallgren, P.H., Swoboda-Colberg, N.G., Liu, F. and Colberg, P.J. (2012) Electrochemical depassivation of zero-valent iron for trichloroethene reduction. *J. Hazard. Mater.* 239, 265-269.
- Coles, C.A., Rao, S.R. and Yong, R.N. (2000) Lead and cadmium interactions with mackinawite: Retention mechanisms and the role of pH. *Environ. Sci. Technol.* 34(6), 996-1000.
- Crane, R., Dickinson, M., Popescu, I. and Scott, T. (2011) Magnetite and zero-valent iron nanoparticles for the remediation of uranium contaminated environmental water. *Water Res.* 45(9), 2931-2942.
- Cundy, A.B., Hopkinson, L. and Whitby, R.L. (2008) Use of iron-based technologies in contaminated land and groundwater remediation: a review. *Sci. Total Environ.* 400(1), 42-51.
- Dries, J., Bastiaens, L., Springael, D., Kuypers, S., Agathos, S.N. and Diels, L. (2005) Effect of humic acids on heavy metal removal by zero-valent iron in batch and continuous flow column systems. *Water Res.* 39(15), 3531-3540.
- Du, J., Bao, J., Lu, C. and Werner, D. (2016) Reductive sequestration of chromate by hierarchical FeS@ Fe⁰ particles. *Water Res.* 102, 73-81.

- Enning, D. and Garrelfs, J. (2014) Corrosion of iron by sulfate-reducing bacteria: new views of an old problem. *Applied and environmental microbiology* 80(4), 1226-1236.
- Fan, D., Anitori, R.P., Tebo, B.M., Tratnyek, P.G., Lezama Pacheco, J.S., Kukkadapu, R.K., Engelhard, M.H., Bowden, M.E., Kovarik, L. and Arey, B.W. (2013) Reductive sequestration of pertechnetate ($^{99}\text{TcO}_4^-$) by nano zero-valent iron (nZVI) transformed by abiotic sulfide. *Environ. Sci. Technol.* 47(10), 5302-5310.
- Fan, D., Lan, Y., Tratnyek, P.G., Johnson, R.L., Filip, J., O'Carroll, D.M., Nunez Garcia, A. and Agrawal, A. (2017) Sulfidation of Iron-Based Materials: A Review of Processes and Implications for Water Treatment and Remediation. *Environ. Sci. Technol.* 51(22), 13070-13085.
- Fan, D., O'Brien Johnson, G., Tratnyek, P.G. and Johnson, R.L. (2016) Sulfidation of nano zerovalent iron (nZVI) for improved selectivity during in-situ chemical reduction (ISCR). *Environ. Sci. Technol.* 50(17), 9558-9565.
- Fendorf, S.E. and Li, G. (1996) Kinetics of chromate reduction by ferrous iron. *Environ. Sci. Technol.* 30(5), 1614-1617.
- Feng, P., Guan, X., Sun, Y., Choi, W., Qin, H., Wang, J., Qiao, J. and Li, L. (2015) Weak magnetic field accelerates chromate removal by zero-valent iron. *Journal of Environmental Sciences* 31, 175-183.
- Fu, F., Dionysiou, D.D. and Liu, H. (2014) The use of zero-valent iron for groundwater remediation and wastewater treatment: a review. *J. Hazard. Mater.* 267, 194-205.
- Galicía, L., Gonzalez, I., Meas, Y. and Ibañez, J.G. (1990) Pourbaix-type diagram of Fe (III) and Fe (II) phenanthroline complexes. *Electrochim. Acta* 35(1), 209-213.
- Gheju, M. (2011) Hexavalent chromium reduction with zero-valent iron (ZVI) in aquatic systems. *Water, Air, & Soil Pollution* 222(1-4), 103-148.
- Gheju, M. and Iovi, A. (2006) Kinetics of hexavalent chromium reduction by scrap iron. *J. Hazard. Mater.* 135(1), 66-73.
- Gong, Y., Tang, J. and Zhao, D. (2016) Application of iron sulfide particles for groundwater and soil remediation: a review. *Water Res.* 89, 309-320.
- Gu, B., Phelps, T., Liang, L., Dickey, M., Roh, Y., Kinsall, B., Palumbo, A. and Jacobs, G. (1999) Biogeochemical dynamics in zero-valent iron columns: implications for permeable reactive barriers. *Environ. Sci. Technol.* 33(13), 2170-2177.
- Gu, Y., Wang, B., He, F., Bradley, M.J. and Tratnyek, P.G. (2017) Mechanochemically sulfidated microscale zero valent iron: Pathways, kinetics, mechanism, and efficiency of trichloroethylene dechlorination. *Environ. Sci. Technol.* 51(21), 12653-12662.
- Guan, X., Sun, Y., Qin, H., Li, J., Lo, I.M., He, D. and Dong, H. (2015) The limitations of applying zero-valent iron technology in contaminants sequestration and the corresponding countermeasures: the development in zero-valent iron technology in the last two decades (1994–2014). *Water Res.* 75, 224-248.
- Han, Y.-S., Jeong, H.Y., Demond, A.H. and Hayes, K.F. (2011) X-ray absorption and photoelectron spectroscopic study of the association of As (III) with nanoparticulate FeS and FeS-coated sand. *Water Res.* 45(17), 5727-5735.
- Han, Y. and Yan, W. (2016) Reductive Dechlorination of trichloroethene by zero-valent iron nanoparticles: Reactivity enhancement through sulfidation treatment. *Environ. Sci. Technol.* 50(23), 12992-13001.
- Hyun, S.P., Davis, J.A., Sun, K. and Hayes, K.F. (2012) Uranium(VI) reduction by iron(II) monosulfide mackinawite. *Environ. Sci. Technol.* 46(6), 3369-3376.

- Icenhower, J.P., Qafoku, N.P., Zachara, J.M. and Martin, W.J. (2010) The biogeochemistry of technetium: a review of the behavior of an artificial element in the natural environment. *American Journal of Science* 310(8), 721-752.
- Jeong, H.Y., Han, Y.-S., Park, S.W. and Hayes, K.F. (2010a) Aerobic oxidation of mackinawite (FeS) and its environmental implication for arsenic mobilization. *Geochim. Cosmochim. Acta* 74(11), 3182-3198.
- Jeong, H.Y., Sun, K. and Hayes, K.F. (2010b) Microscopic and spectroscopic characterization of Hg(II) immobilization by mackinawite (FeS). *Environ. Sci. Technol.* 44(19), 7476-7483.
- Joo, S.H., Feitz, A.J., Sedlak, D.L. and Waite, T.D. (2005) Quantification of the oxidizing capacity of nanoparticulate zero-valent iron. *Environ. Sci. Technol.* 39(5), 1263-1268.
- Keenan, C.R. and Sedlak, D.L. (2008) Factors affecting the yield of oxidants from the reaction of nanoparticulate zero-valent iron and oxygen. *Environ. Sci. Technol.* 42(4), 1262-1267.
- Kim, D.-h., Kim, J. and Choi, W. (2011) Effect of magnetic field on the zero valent iron induced oxidation reaction. *J. Hazard. Mater.* 192(2), 928-931.
- Kim, E.-J., Murugesan, K., Kim, J.-H., Tratnyek, P.G. and Chang, Y.-S. (2013) Remediation of trichloroethylene by FeS-coated iron nanoparticles in simulated and real groundwater: Effects of water chemistry. *Industrial & Engineering Chemistry Research* 52(27), 9343-9350.
- Kirschling, T.L., Gregory, K.B., Minkley, J., Edwin G, Lowry, G.V. and Tilton, R.D. (2010) Impact of nanoscale zero valent iron on geochemistry and microbial populations in trichloroethylene contaminated aquifer materials. *Environ. Sci. Technol.* 44(9), 3474-3480.
- Lee, C. (2015) Oxidation of organic contaminants in water by iron-induced oxygen activation: A short review. *Environmental Engineering Research* 20(3), 205-211.
- Li, D., Mao, Z., Zhong, Y., Huang, W., Wu, Y. and Peng, P.a. (2016) Reductive transformation of tetrabromobisphenol A by sulfidated nano zerovalent iron. *Water Res.* 103, 1-9.
- Li, D., Zhu, X., Zhong, Y., Huang, W. and Peng, P.a. (2017a) Abiotic transformation of hexabromocyclododecane by sulfidated nanoscale zerovalent iron: Kinetics, mechanism and influencing factors. *Water Res.*
- Li, J., Zhang, X., Sun, Y., Liang, L., Pan, B., Zhang, W. and Guan, X. (2017b) Advances in Sulfidation of Zerovalent Iron for Water Decontamination. *Environ. Sci. Technol.* 51(23), 13533-13544.
- Li, S., Wang, W., Liang, F. and Zhang, W.-x. (2017c) Heavy metal removal using nanoscale zero-valent iron (nZVI): Theory and application. *J. Hazard. Mater.* 322, 163-171.
- Li, S., Wang, W., Liu, Y. and Zhang, W.-x. (2014a) Zero-valent iron nanoparticles (nZVI) for the treatment of smelting wastewater: A pilot-scale demonstration. *Chem. Eng. J.* 254, 115-123.
- Li, S., Wang, W., Yan, W. and Zhang, W.-x. (2014b) Nanoscale zero-valent iron (nZVI) for the treatment of concentrated Cu (II) wastewater: a field demonstration. *Environmental Science: Processes & Impacts* 16(3), 524-533.
- Li, Y., Li, J. and Zhang, Y. (2012) Mechanism insights into enhanced Cr (VI) removal using nanoscale zerovalent iron supported on the pillared bentonite by macroscopic and spectroscopic studies. *J. Hazard. Mater.* 227, 211-218.
- Liang, L., Guan, X., Huang, Y., Ma, J., Sun, X., Qiao, J. and Zhou, G. (2015) Efficient selenate removal by zero-valent iron in the presence of weak magnetic field. *Sep. Purif. Technol.* 156, 1064-1072.
- Liang, L., Guan, X., Shi, Z., Li, J., Wu, Y. and Tratnyek, P.G. (2014a) Coupled effects of aging and weak magnetic fields on sequestration of selenite by zero-valent iron. *Environ. Sci. Technol.* 48(11), 6326-6334.

- Liang, L., Sun, W., Guan, X., Huang, Y., Choi, W., Bao, H., Li, L. and Jiang, Z. (2014b) Weak magnetic field significantly enhances selenite removal kinetics by zero valent iron. *Water Res.* 49, 371-380.
- Liang, L., Yang, W., Guan, X., Li, J., Xu, Z., Wu, J., Huang, Y. and Zhang, X. (2013) Kinetics and mechanisms of pH-dependent selenite removal by zero valent iron. *Water Res.* 47(15), 5846-5855.
- Liu, T., Li, X. and Waite, T.D. (2013a) Depassivation of aged Fe⁰ by ferrous ions: Implications to contaminant degradation. *Environ. Sci. Technol.* 47(23), 13712-13720.
- Liu, T., Li, X. and Waite, T.D. (2013b) Depassivation of aged Fe⁰ by inorganic salts: Implications to contaminant degradation in seawater. *Environ. Sci. Technol.* 47(13), 7350-7356.
- Mamindy-Pajany, Y., Hurel, C., Marmier, N. and Roméo, M. (2011) Arsenic (V) adsorption from aqueous solution onto goethite, hematite, magnetite and zero-valent iron: effects of pH, concentration and reversibility. *Desalination* 281, 93-99.
- McBeth, J., Lloyd, J., Law, G., Livens, F., Burke, I. and Morris, K. (2011) Redox interactions of technetium with iron-bearing minerals. *Mineralogical Magazine* 75(4), 2419-2430.
- Mu, Y., Ai, Z. and Zhang, L. (2017) Phosphate Shifted Oxygen Reduction Pathway on Fe@Fe₂O₃ Core-Shell Nanowires for Enhanced Reactive Oxygen Species Generation and Aerobic 4-Chlorophenol Degradation. *Environ. Sci. Technol.* 51(14), 8101-8109.
- Mu, Y., Ai, Z., Zhang, L. and Song, F. (2015) Insight into core-shell dependent anoxic Cr (VI) removal with Fe@ Fe₂O₃ nanowires: Indispensable role of surface bound Fe (II). *ACS applied materials & interfaces* 7(3), 1997-2005.
- Newman, R.C., Rumash, K. and Webster, B.J. (1992) The effect of pre-corrosion on the corrosion rate of steel in neutral solutions containing sulphide: Relevance to microbially influenced corrosion. *Corros. Sci.* 33(12), 1877-1884.
- O'Loughlin, E.J., Boyanov, M.I., Antonopoulos, D.A. and Kemner, K.M. (2011) *Aquatic Redox Chemistry*, pp. 477-517, ACS Publications.
- Phillips, D.H., Nooten, T.V., Bastiaens, L., Russell, M., Dickson, K., Plant, S., Ahad, J., Newton, T., Elliot, T. and Kalin, R. (2010) Ten year performance evaluation of a field-scale zero-valent iron permeable reactive barrier installed to remediate trichloroethene contaminated groundwater. *Environ. Sci. Technol.* 44(10), 3861-3869.
- Ponder, S.M., Darab, J.G. and Mallouk, T.E. (2000) Remediation of Cr (VI) and Pb (II) aqueous solutions using supported, nanoscale zero-valent iron. *Environ. Sci. Technol.* 34(12), 2564-2569.
- Powell, B.A., Fjeld, R.A., Kaplan, D.I., Coates, J.T. and Serkiz, S.M. (2004) Pu (V) O₂⁺ adsorption and reduction by synthetic magnetite (Fe₃O₄). *Environ. Sci. Technol.* 38(22), 6016-6024.
- Powell, R.M., Puls, R.W., Hightower, S.K. and Sabatini, D.A. (1995) Coupled iron corrosion and chromate reduction: mechanisms for subsurface remediation. *Environ. Sci. Technol.* 29(8), 1913-1922.
- Puls, R.W., Paul, C.J. and Powell, R.M. (1999) The application of in situ permeable reactive (zero-valent iron) barrier technology for the remediation of chromate-contaminated groundwater: A field test. *Appl. Geochem.* 14(81), 989-1000.
- Qin, H., Li, J., Bao, Q., Li, L. and Guan, X. (2016) Role of dissolved oxygen in metal (loid) removal by zerovalent iron at different pH: its dependence on the removal mechanisms. *RSC Advances* 6(55), 50144-50152.

- Qin, H., Li, J., Yang, H., Pan, B., Zhang, W. and Guan, X. (2017) Coupled Effect of Ferrous Ion and Oxygen on the Electron Selectivity of Zerovalent Iron for Selenate Sequestration. *Environ. Sci. Technol.* 51(9), 5090-5097.
- Rai, D., Eary, L. and Zachara, J. (1989) Environmental chemistry of chromium. *Sci. Total Environ.* 86(1-2), 15-23.
- Rajajayavel, S.R.C. and Ghoshal, S. (2015) Enhanced reductive dechlorination of trichloroethylene by sulfidated nanoscale zerovalent iron. *Water Res.* 78, 144-153.
- Ramos, M.A., Yan, W., Li, X.-q., Koel, B.E. and Zhang, W.-x. (2009) Simultaneous oxidation and reduction of arsenic by zero-valent iron nanoparticles: Understanding the significance of the core-shell structure. *The Journal of Physical Chemistry C* 113(33), 14591-14594.
- Scherer, M.M., Balko, B.A. and Tratnyek, P.G. (1998), ACS Publications.
- Sedlak, D.L. and Chan, P.G. (1997) Reduction of hexavalent chromium by ferrous iron. *Geochim. Cosmochim. Acta* 61(11), 2185-2192.
- Shipley, H.J., Yean, S., Kan, A.T. and Tomson, M.B. (2010) A sorption kinetics model for arsenic adsorption to magnetite nanoparticles. *Environmental Science and Pollution Research* 17(5), 1053-1062.
- Su, Y., Adeleye, A.S., Keller, A.A., Huang, Y., Dai, C., Zhou, X. and Zhang, Y. (2015) Magnetic sulfide-modified nanoscale zerovalent iron (S-nZVI) for dissolved metal ion removal. *Water Res.* 74, 47-57.
- Sun, W. and Nešić, S. (2009) A mechanistic model of uniform hydrogen sulfide/carbon dioxide corrosion of mild steel. *Corrosion* 65(5), 291-307.
- Sun, Y., Li, J., Huang, T. and Guan, X. (2016) The influences of iron characteristics, operating conditions and solution chemistry on contaminants removal by zero-valent iron: A review. *Water Res.* 100, 277-295.
- Tang, C., Huang, Y.H., Zeng, H. and Zhang, Z. (2014) Reductive removal of selenate by zero-valent iron: The roles of aqueous Fe 2+ and corrosion products, and selenate removal mechanisms. *Water Res.* 67, 166-174.
- Turcio-Ortega, D., Fan, D., Tratnyek, P.G., Kim, E.-J. and Chang, Y.-S. (2012) Reactivity of Fe/FeS nanoparticles: Electrolyte composition effects on corrosion electrochemistry. *Environ. Sci. Technol.* 46(22), 12484-12492.
- Um, W., Chang, H.-S., Icenhower, J.P., Lukens, W.W., Serne, R.J., Qafoku, N.P., Westsik Jr, J.H., Buck, E.C. and Smith, S.C. (2011) Immobilization of 99-technetium (VII) by Fe (II)-goethite and limited reoxidation. *Environ. Sci. Technol.* 45(11), 4904-4913.
- Xie, Y. and Cwiertny, D.M. (2010) Use of dithionite to extend the reactive lifetime of nanoscale zero-valent iron treatment systems. *Environ. Sci. Technol.* 44(22), 8649-8655.
- Xu, C., Zhang, B., Wang, Y., Shao, Q., Zhou, W., Fan, D., Bandstra, J.Z., Shi, Z. and Tratnyek, P.G. (2016a) Effects of Sulfidation, Magnetization, and Oxygenation on Azo Dye Reduction by Zerovalent Iron. *Environ. Sci. Technol.* 50(21), 11879-11887.
- Xu, C., Zhang, B., Zhu, L., Lin, S., Sun, X., Jiang, Z. and Tratnyek, P.G. (2016b) Sequestration of antimonite by zerovalent iron: Using weak magnetic field effects to enhance performance and characterize reaction mechanisms. *Environ. Sci. Technol.* 50(3), 1483-1491.
- Xu, P., Zeng, G.M., Huang, D.L., Feng, C.L., Hu, S., Zhao, M.H., Lai, C., Wei, Z., Huang, C. and Xie, G.X. (2012) Use of iron oxide nanomaterials in wastewater treatment: a review. *Sci. Total Environ.* 424, 1-10.
- Xu, Y. and Zhao, D. (2007) Reductive immobilization of chromate in water and soil using stabilized iron nanoparticles. *Water Res.* 41(10), 2101-2108.

- Xue, A., Shen, Z.-Z., Zhao, B. and Zhao, H.-Z. (2013) Arsenite removal from aqueous solution by a microbial fuel cell–zerovalent iron hybrid process. *J. Hazard. Mater.* 261, 621-627.
- Yan, W., Herzing, A.A., Kiely, C.J. and Zhang, W.-x. (2010) Nanoscale zero-valent iron (nZVI): Aspects of the core-shell structure and reactions with inorganic species in water. *J. Contam. Hydrol.* 118(3), 96-104.
- Yoon, I.-H., Bang, S., Chang, J.-S., Kim, M.G. and Kim, K.-W. (2011) Effects of pH and dissolved oxygen on Cr (VI) removal in Fe (0)/H₂O systems. *J. Hazard. Mater.* 186(1), 855-862.
- Zhang, Y., Su, Y., Zhou, X., Dai, C. and Keller, A.A. (2013) A new insight on the core-shell structure of zerovalent iron nanoparticles and its application for Pb (II) sequestration. *J. Hazard. Mater.* 263, 685-693.
- Zheng, Y., Ning, J., Brown, B., Young, D. and Nesic, S. (2015) Mechanistic study of the effect of iron sulfide layers on hydrogen sulfide corrosion of carbon steel, p. 5933, NACE International, Dallas, Texas.
- Zhou, H., He, Y., Lan, Y., Mao, J. and Chen, S. (2008) Influence of complex reagents on removal of chromium (VI) by zero-valent iron. *Chemosphere* 72(6), 870-874.
- Zou, Y., Wang, X., Khan, A., Wang, P., Liu, Y., Alsaedi, A., Hayat, T. and Wang, X. (2016) Environmental remediation and application of nanoscale zero-valent iron and its composites for the removal of heavy metal ions: a review. *Environ. Sci. Technol.* 50(14), 7290-7304.